Oil & Natural Gas Technology

DOE Award No.: DE-FE0013889

Quarterly Research Performance Progress Report (Period ending 03/31/2014)

THCM Coupled Model For Hydrate-Bearing Sediments: Data Analysis and Design of New Field Experiments (Marine and Permafrost Settings)

Project Period (10/1/2013 to 09/30/2015)

Submitted by:

Marcelo Sanchez Project PI

Texas A&M University
DUNS #: 847205572
College Station, TX
979-862-6604
msanchez@civil.tamu

J. Carlos Santamarina

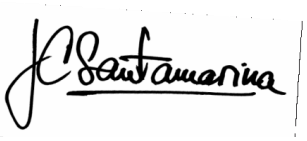

Georgia Institute of Technology
Atlanta, Georgia
404-894-7605
edujcs@gatech.edu

Prepared for:
United States Department of Energy
National Energy Technology Laboratory
Submission date: 01/31/2014

Office of Fossil Energy

DISCLAIMER

ACCOMPLISHMENTS

The experimental study of hydrate bearing sediments has been hindered by the very low solubility of methane in water (lab testing), and inherent sampling difficulties associated with depressurization and thermal changes during core extraction. This situation has prompted more decisive developments in numerical modeling in order to advance the current understanding of hydrate bearing sediments, and to investigate/optimize production strategies and implications. The goals of this research is to addresses the complex thermo-hydro-chemo-mechanical THCM coupled phenomena in hydrate-bearing sediments, using a truly coupled numerical model that incorporates sound and proven constitutive relations, satisfies fundamental conservation principles. This tool will allow us to better analyze available data and to further enhance our understanding of hydrate bearing sediments in view of future field experiments and the development of production technology.

ACCOMPLISHED

The project management plan (PMP, Task 1) and the selection of the PhD Students working during the 1st year of the project were competed and informed in the first quarterly report. The main accomplishments for this first period address Tasks 2, 3 and 4 of the original research plan, and include:

- Student training.
- Literature review.
- Update of constitutive equations.
- Update of THCM-Hydrate.
- Close-form analytical solutions.

Training

The training of the two PhD students working in this project has continued during this period. As for Mr. Xuerui (Gary) Gai (i.e. the Ph.D. student at TAMU) the training activities have been focused on the use of "THCM-Hydrate", the numerical code under development in this project. He is becoming familiar with the operation of this code, constitutive laws; imposition of boundary conditions and other aspects of the numerical code. As Mr. Z Sun (the Ph.D. student at GT), he training has focused on the development of constitutive laws for hydrate bearing sediments (HBS) and analytical solution. Both students have progressed positively with their coursework at their respective universities.

Literature review

The literature review (Task 2a) has been continued during this period, and it includes.

- Published constitutive models for (HBS).
- Analytical and numerical modeling of HBS.
- Laboratory and field investigation related to HBS.

Update of constitutive equations

The update of the constitutive laws for hydrate-bearing marine sediments (Task 2b–ongoing) and HBS in the permafrost (Task 2c – ongoing) have continued during this period.

The section below (page 6) entitled: "Dynamic effects on the capillary pressure-saturation relationship – Relevance to HBS modeling" briefly presents the main findings related to the update of constitutive equations and also some of the activities performed in Task 4.a.

Update of THCM-Hydrate

The update of the numerical code "THCM-Hydrate" has continued during this reporting period. The main following activities for the different subtasks are highlighted:

- Validation of implemented functions (Task 3a – ongoing), including
  - The effect of cryogenic suction on the mechanical behavior of frozen sediments has been studied. The section below (page 13) entitled: "Effect of subzero temperature and cryogenic suction on the mechanical behavior of frozen sediments" briefly present the main research in this subject.
- Synthetic numerical tests (Task 3b – ongoing), including
  - Some of the synthetic numerical tests presented in the previous quarterly report have been modeled.
- Code comparison analyses (Task 3c – ongoing), including
  - We have started with the simulations aimed at comparing our code against other ones developed to model the behavior of HBS. We are using the benchmark exercises prepared in the context of "The National Methane Hydrates R&D Program: Methane Hydrate Reservoir Simulator Code Comparison Study" (http://www.netl.doe.gov/technologies/oil-gas/FutureSupply/MethaneHydrates/MH_CodeCompare/MH_CodeCompare.html
  - We have already informed in previous report about the successful completion of Benchmark Test # 1. We are currently working on Benchmark Test # 2 and 3.

Close-form analytical solutions

A review on the main governing evolution laws, parameters, dimensionless ratios and simplifying assumptions for HBS dissociation has been started. A brief summary of those activities (i.e. Task 4.a) is presented in the section below (page 6) entitled: "Dynamic effects on the capillary pressure-saturation relationship – Relevance to HBS modeling".

Plan - Next reporting period

We will advance analytical and numerical fronts to enhance our code to solve coupled THCM problems involving with HBS, with renewed emphasis on simulating the natural processes under *in-situ* conditions and gas production.

Milestones for each budget period of the project are tabulated next. These milestones are selected to show progression towards project goals.

	Milestone Title Planned Date and Verification Method	Actual Completion Date	Comments
Title Related Task / Subtasks Planned Date Verification method	Complete literature review 2.0 / 2.a March 2014 Report	March 2014	Progressing as planned
Title Related Task / Subtasks Planned Date Verification method	Complete updated Constitutive Equations 2.0 / 2.b & 2.c June 2014 Report (with preliminary validation data)	June 2014	Progressing as planned
Title Related Task / Subtasks Planned Date Verification method	Validate new THCM constitutive equations 3.0 / 3.a, 3.b & 3.c September 2014 Report (with first comparisons between experimental and numerical results)	September 2014	Progressing as planned
Title Related Task / Subtasks Planned Date Verification method	Complete close-form analytical solutions 4.0 / 4.a & 4.b February 2015 Report (with analytical data)	February 2015	Progressing as planned
Title Related Task / Subtasks Planned Date Verification method	Complete numerical analyses 5.0 / 5.a, 5.b & 5.c July 2015 Report (with analytical and numerical data)	July 2015	Activities not started yet
Title Related Task / Subtasks Planned Date Verification method	Complete THCM-Hydrate code modifications 6.0 / 6.a June 2015 Report (with numerical data)	June 2015	Activities not started yet
Title Related Task / Subtasks Planned Date Verification method	Complete production optimization 7.0 / 7.a, 7.b, 7.c, 7.d & 7.e September 2015 Report (with numerical data)	September 2015	Activities not started yet

DYNAMIC EFFECTS ON THE CAPILLARY PRESSURE-SATURATION RELATIONSHIP – RELEVANCE TO HBS MODELING.

Pressure-saturation relationships in unsaturated sediments

The capillary pressure-saturation relationship, also known as soil-water characteristic curve or soil water retention curve, defines the relationship between capillary pressure and degree of saturation. This relationship plays a central role in modeling unsaturated soil behavior. Pressure-saturation data contains information about the soil structure, pore size distribution and pore connectivity (Barbour, 1998). Consequently, the soil water characteristic curve affects the evolution of strains and mixed-fluid conductivity (van Genuchten, 1980; Fredlund, 2000; Vanapalli et al., 1996). Traditional solutions to two-phase flow in porous media impose mass conservation and Darcy's law (Bottero, 2009):

Mass conservation for wetting phase (water):

$$\frac{\partial \phi \rho_w S_w}{\partial t} - \nabla \cdot \left[\frac{\rho_w k_{rw} \mathbf{K}}{\mu_w} \left(\nabla P_w - \rho_w \mathbf{g} \right) \right] = 0 \tag{1}$$

Mass conservation for nonwetting phase (gas):

$$\frac{\partial \phi \rho_g S_g}{\partial t} - \nabla \cdot \left[\frac{\rho_g k_{rg} \mathbf{K}}{\mu_g} \left(\nabla P_g - \rho_g \mathbf{g} \right) \right] = 0 \tag{2}$$

Constraint:

$$S_w + S_g = 1 \tag{3}$$

where ϕ is porosity; $\mathbf{K}$ is the intrinsic permeability; ρ_g and ρ_w are the densities of the gas and water, respectively; S_g and S_w are the partial saturations of gas and water, respectively; P_g and P_w are the gas and water phase pressures, respectively; μ_g and μ_w are the viscosities of the gas and water, respectively; t is the time; and $\mathbf{g}$ is the gravity vector (0,0,-g) . The capillary pressure-saturation relationship is the fourth equation needed to solve the coupled problem:

$$P_g - P_w = P_c(S_w) \tag{4}$$

These four equations combine into two PDEs and are numerically solved (Celia et al., 1992; Kueper and Frind, 1991). Table 1 lists commonly used capillary pressure-saturation and relative permeability-saturation relationships.

Table 1. Commonly used capillary pressure-saturation and relative permeability-saturation relationships

Capillary pressure-saturation relationship	Relative permeability-saturation relationship	Reference
$P_c(S_e) = P_d \cdot S_e^{-1/\lambda}$	$k_{rw} = S_e^{3+2/\lambda}$ $k_{rg} = (1-S_e)^2\left(1-S_e^{1+2/\lambda}\right)$	Corey (1994)
$P_c(S_e) = P_0(S_e^{-1/m}-1)^{1/n}$	$k_{rw} = S_e^{1/2}\cdot\left[1-\left(1-S_e^{1/m}\right)^m\right]^2$ $k_{rg} = (1-S_e)^{1/2}\cdot\left(1-S_e^{1/m}\right)^{2m}$ ($m=1-1/n$)	Mualem (1976), van Genuchten (1980)
$P_c(S_e) = \gamma\sqrt{\frac{\phi}{K}}J(S_e)$		Leverett (1941)

Parameters: S_e is effective saturation, P_d represents air entry pressure, λ indicates pore size distribution index; P_0 represents the air entry pressure; γ is surface tension, K is intrinsic permeability, ϕ is porosity, $J(S_e)$ is a dimensionless function of saturation (Vereecken et al., 2007). Parameters in relative permeability-saturation relationship are corresponding to those in capillary pressure-saturation relationship.

Current use of the capillary pressure-saturation relationship in HBS studies

Capillary pressure-saturation relationships play a central role in HBS modelling (Rutqvist and Moridis, 2009; Sanchez et al., 2013; Klar et al., 2010; Kimoto et al., 2007). Table 2 lists capillary pressure-saturation models and relative permeability-saturation models used in HBS simulations. The presence of hydrate in the pore space is recognized through a redefinition of effective saturation (Klar et al., 2010; Kimoto et al., 2007; Sun et al. 2005; Moridis and Sloan, 2007):

$$S_e = \frac{S_w - S_r}{1 - S_r - S_h} \tag{5}$$

where S_r and S_h are is residual and hydrate saturation (detailed discussion in Jang and Santamarina 2014). Hydrate dissociation is included as a source in flow equations:

$$\frac{\partial \phi \rho_w S_w}{\partial t} - \nabla \cdot \left[\frac{\rho_w k_{rw} \mathbf{K}_{hbs}}{\mu_w}\left(\nabla P_w - \rho_w \mathbf{g}\right)\right] - \dot{m}_w = 0 \tag{6}$$

$$\frac{\partial \phi \rho_g S_g}{\partial t} - \nabla \cdot \left[\frac{\rho_g k_{rg} \mathbf{K}_{hbs}}{\mu_g}\left(\nabla P_g - \rho_g \mathbf{g}\right)\right] - \dot{m}_g = 0 \tag{7}$$

$$\dot{m}_h = -\dot{m}_g - \dot{m}_w \tag{8}$$

where $\dot{m}$ is the mass change due to hydrate dissociation (w:for water; g:gas; h:hydrate).

Table 2. Capillary pressure-saturation and relative permeability-saturation relationships used in HBS modeling.

Reference	Capillary pressure model	Relative permeability model
Liu and Flemings (2007)	J-function	Corey model
Sun et al. (2005)	Brook and Corey (1964)	Corey model
Klar et al (2010)	van Genuchten (1980)	Mualem (1976)
Kimoto et al (2007)	van Genuchten (1980)	No relative permeability
Moridis and Sloan (2007)	van Genuchten (1980)	Corey model
Sanchez et al. (2013)	van Genuchten (1980)	Mualem (1976)

Limitations in current models

The current use of capillary pressure-saturation relationships in HBS modelling faces three limitations. First, it does not consider the change of pore size distribution due to the presence of hydrate, as hydrates occupy large pores (Dai and Santamarina, 2013). Second, the dissociation of hydrate is a non-equilibrium process while traditional capillary pressure-saturation relationships represent equilibrium conditions (O'Carroll et al., 2005; Diamantopoulos et al., 2012b; Ross and Smettem, 2000). Third, the low viscosity ratio between gas and water may cause fingered gas invasion (Santamarina and Jang, 2011).

Finally, it should also be noted that the evolution of relative water and gas permeabilities in hydrate bearing sediments requires further research (Ruan et al., 2012; Anderson et al., 2011; Kumar et al., 2010). Overall, physical models and experimental studies show that hydrate pore habit can have a pronounced effect on conductivity properties (Kumar et al, 2010; Johnson et al., 2011; Seol and Kneafsey, 2011). This last observation can be extended to pressure-saturation trends as well as.

Dynamic effects on pressure-saturation trends

The capillary pressure-saturation relationship is experimentally determined under equilibrium conditions. Outside equilibrium, pressure-saturation becomes flow-rate dependent (a.k.a., dynamic effect, nonuniqueness, or nonequilibrium - Hassanizadeh et al., 2002; Diamantopoulos et al., 2012a).

Observations. Drainage experiments conducted on sand columns under static, steady-state and transient conditions show clear differences in pressure-saturation (Topp et al., 1967; Hassanizadeh et al., 2002; Diamantopoulos et al., 2012). Figure 1 shows the capillary pressure-saturation relationship at the center of columns under different flow conditions (water content measured by gamma ray attenuation and pressure head measured using a tensiometer): at a certain capillary pressure, more water is retained in soils when drainage and gas invasion happen in a short time than in quasi-static equilibrium.

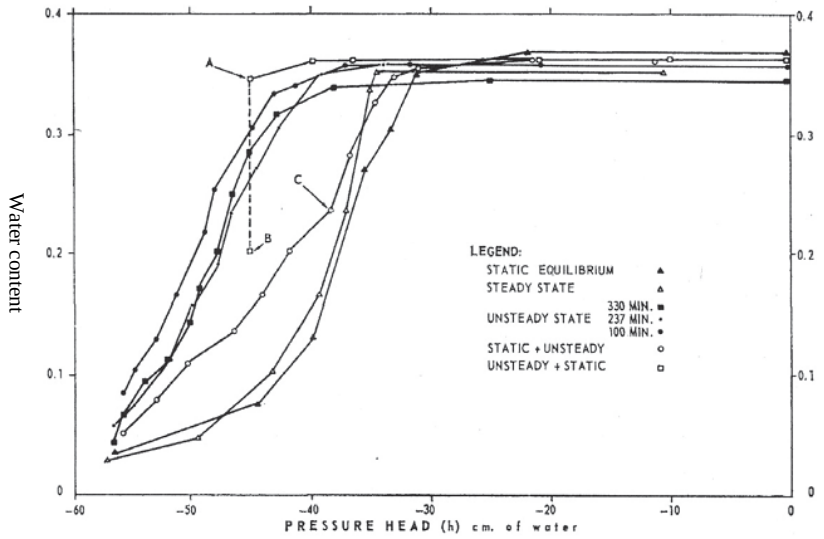

Figure 1. Water content-pressure head data for drainage experiments by Topp et al. (1967 - from Hassanizadeh et al., 2002).

One-step and multistep outflow experiments conducted using sandy and silty soils showed dynamic effects in sandy soils (more water retained in specimens subjected to a higher pressure ramp) but no apparent effects in silty soils (Wildenschild et al., 2001). Furthermore, results showed that traditional two-phase flow models failed to predict the process of outflow in multistep outflow experiments; in particular, flow equilibration takes longer in experiments than in simulations conducted with fitted parameters obtained from steady state capillary pressure-saturation relationship fitted to experimental measurements (Figure 2a - O'Carroll et al., 2005 – see similar dynamic effect results in Das and Mirzaei, 2012; Bottero et al., 2011; Wildenschild et al., 2005; Schultze et al., 1999; Diamantopoulos et al., 2012b).

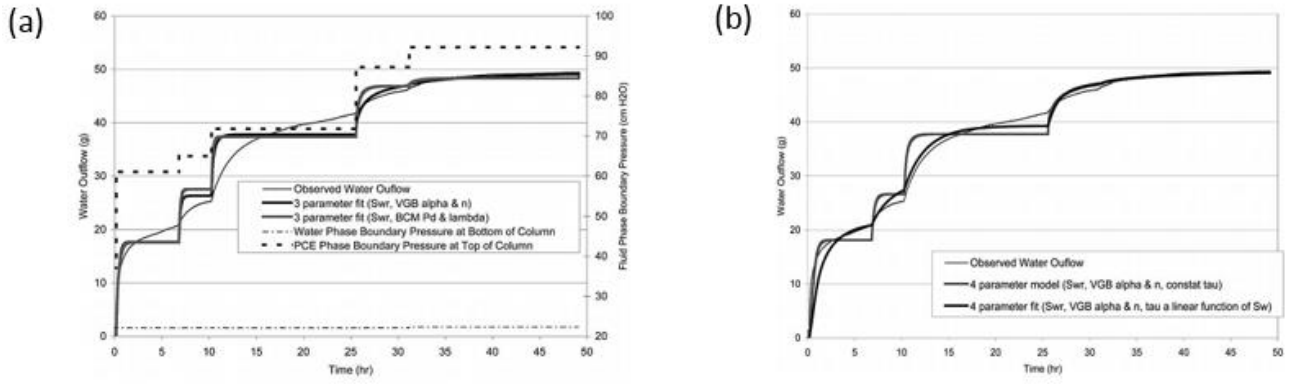

Figure 2. Comparison of observed and fitted cumulative water outflow for multistep outflow, (a) models without dynamic correction; (b) models with dynamic correction (O'Carroll et al., 2005).

Model 1: Dynamic capillary pressure = function of desaturation rate. Experimental results like those presented above led to the inclusion of a dynamic coefficient τ (Hassanizadeh and Gray, 1993; Hassanizadeh et al., 2002):

$$P_c^{dyn} - P_c^{stat} = -\tau \frac{dS}{dt} \tag{9}$$

where the dynamic capillary pressure P_c^{dyn} is the pressure difference between the nonwetting and the wetting phases under dynamic conditions, and S is the degree of saturation. The dynamic coefficient τ captures the speed in saturation change (Bottero et al., 2011; Das and Mirzaei, 2012). Preliminary data suggest that (1) this coefficient varies in orders of magnitude (probably 10^4-10^9 Pa s), (2) it is affected by saturation, fluid properties, pore size distribution, and heterogeneity (Joekar-Niasar and Hassanizadeh, 2011; Mirzaei and Das, 2007), and (3) may be scale-dependent, increasing for larger problems (Bottero et al., 2011; Dahle et al., 2005).

Model 2: Dynamic water content = function of desaturation rate. A relationship between the actual water content and the desaturation rate can also capture dynamic effects observed in experimental results (Ross and Smettem, 2000):

$$\frac{\theta - \theta_{eq}}{\tau} = -\frac{\partial \theta}{\partial t} \tag{10}$$

where θ and θ_{eq} are current and equilibrium water contents, and τ represents the equilibration time. This expression also predicts higher water content in transient conditions than in equilibrium conditions.

Comparison. The two models can be implemented to capture similar effects in single and multi-step outflow processes (O'Carroll et al., 2005; Diamantopoulos et al., 2012).

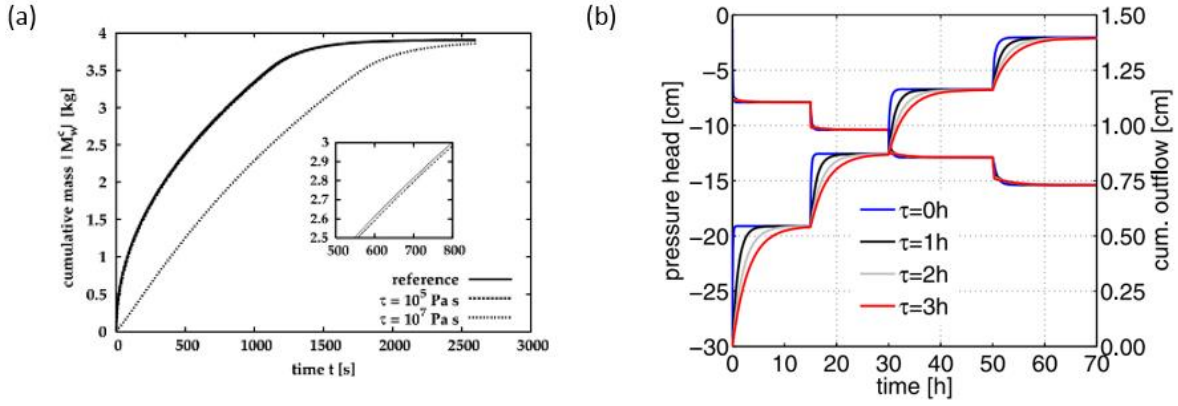

Figure 3. Influence of dynamic coefficient (a) and equilibrium time (b) on predicted outflow (Manthey et al., 2008; Diamantopoulos et al., 2012).

Dynamic effect of capillary pressure-saturation relationship and fingered flow

Fingered flow may bypass most of the matrix, either by focusing on cracks and macropores, or due to flow instability (Gerke et al. 2010). Flow instability may be either gravity-driven or viscosity-driven when a less viscous fluid displaces a more viscous fluid (Homsy, 1987; Nieber et al., 2005; Liu et al., 1994; Glass et al., 1989).

Gravity-driven fingered flow can be simulated by introducing dynamic and hysteretic effects into flow equations (Chapwanya and Stockie, 2010; Sander et al., 2008). Figure 4 shows the influence of dynamic effect and hysteretic effect on flow.

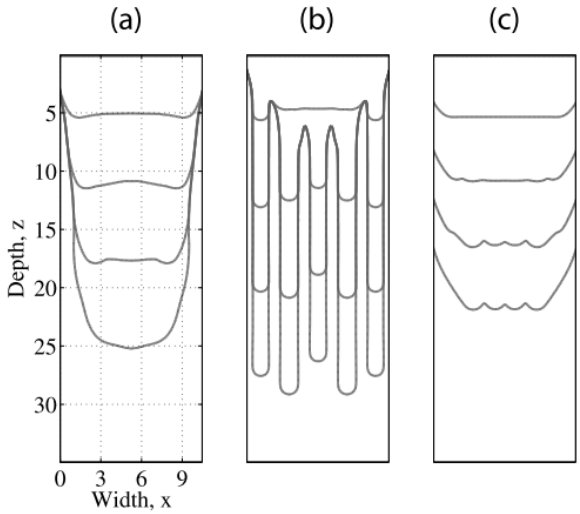

Figure 4. Dynamic and hysteretic effects on flow. a) with hysteretic effect only; b) with both hysteretic and dynamic effects; c) with dynamic effect only (Chapwanya and Stockie, 2010).

Dynamic effects in viscosity-driven fingered flow are often observed in Hele-Shaw cells (e.g., Lovoll et al., 2011). The flow pattern is capillary-controlled in quasi-static experiments (Figure 5). Under dynamic conditions, the displacement pattern reflects viscous fingering at the global scale, but capillary fingering at the pore-scale (figure 6). The crossover length of displacement decreases as the capillary number increases. The transition length-scale is $l_c=a/Ca$, where a is the pore size and Ca is the capillary number. Results obtained under dynamic conditions show higher water retention and residual water content at any given capillary pressure.

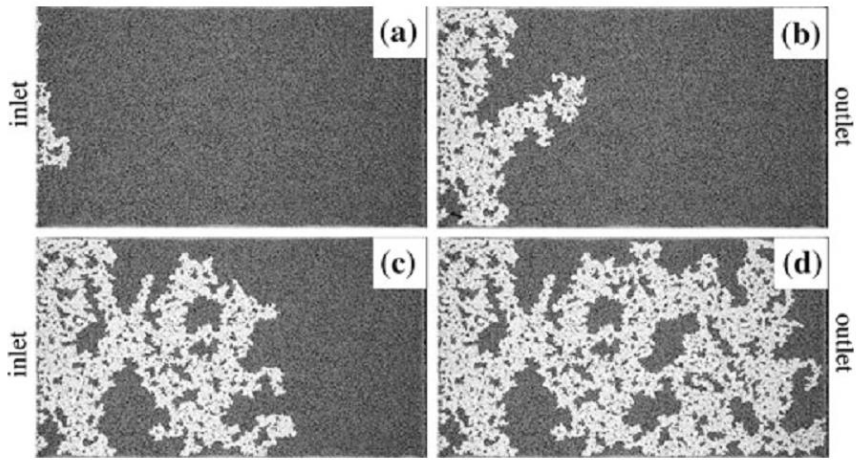

Figure 5. Quasi static drainage experiments (Lovoll et al., 2011)

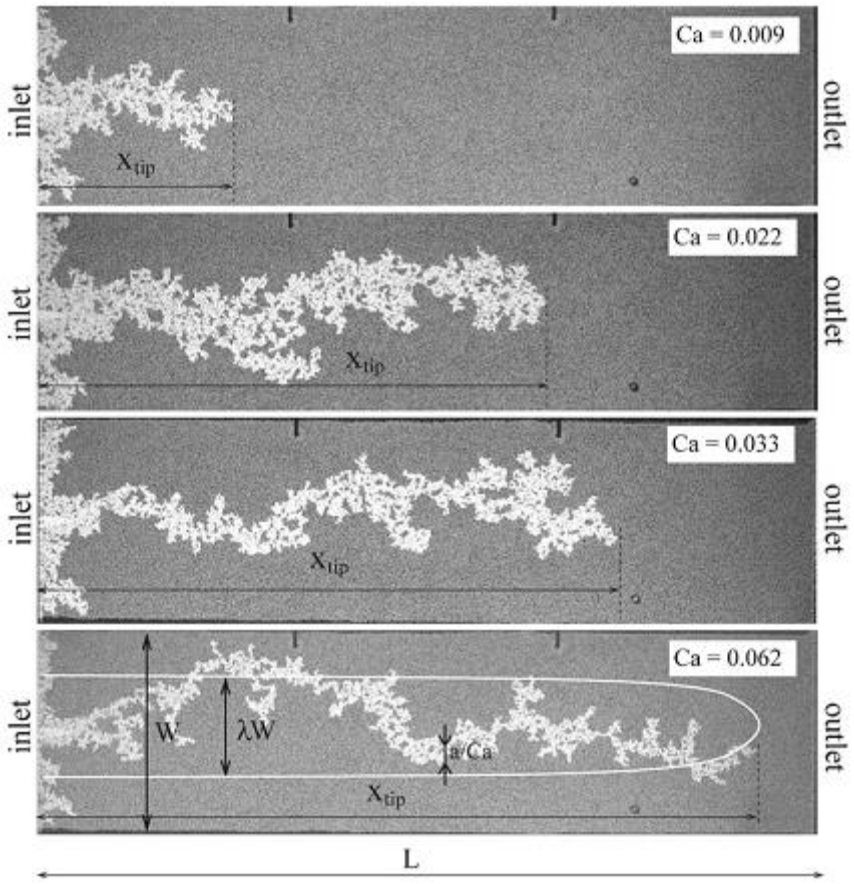

Figure 6. Dynamic drainage experiments - Different capillary numbers (Lovoll et al., 2011).

EFFECT OF SUBZERO TEMPERATURE AND CRYOGENIC SUCTION ON THE MECHANICAL BEHAVIOR OF FROZEN SEDIMENTS.

The primary motivations for the study of frozen soils stemmed from the problems associated with heaving. It was originally thought that the volume changes observed when soils froze were primarily due to the volumetric expansion of water during its phase change to ice. However, the observed volumetric strains greatly differed from the expected ones and that the soils continued to heave if they had access to free water. These observations demanded a revision in this theory. Taber (1929) explained that not all the pore water present in the soil freezes when the temperature reduces below the freezing point of water and termed this as 'unfrozen water'. The presence of this unfrozen water was mainly attributed to a capillary action of the pore spaces in the soils. Beskow (1935) observed that larger pores freeze at higher temperatures when compared to smaller one. The concept of unfrozen water was used to develop several constitutive models (Miller, 1978; Konrad & Morgenstern, 1980). The experimental evidence for this unfrozen water was provided in Tice et al. (1988), who used the pulse nuclear magnetic resonance technique. Other methods such as the dilatometer technique, cation exchange (Tice et al., 1976), electron microscope (White, 1999), were also developed to demonstrate the presence of unfrozen water in frozen soils. These techniques concentrated mainly on clays where the unfrozen water influences the microstructure behavior. Larger pores were observed to freeze at higher temperature compared to smaller pores and this effect was attributed to the capillary action in the pores.
Several models recognize a critical radius of the pore for freezing to occur at a given temperature (Multon et. al, 2012). The schematic representation of the soil structure with the ice and unfrozen water is shown in Figure 7.a). Equilibrium is formed between the unfrozen water and the ice present in the pore space. This equilibrium is quantified using the cryogenic suction (difference of the ice and unfrozen liquid pressure) and is seen to have important changes in the behavior of ice rich soils. Figure 7.b shows a schematic representation of the capillary in frozen sediments.

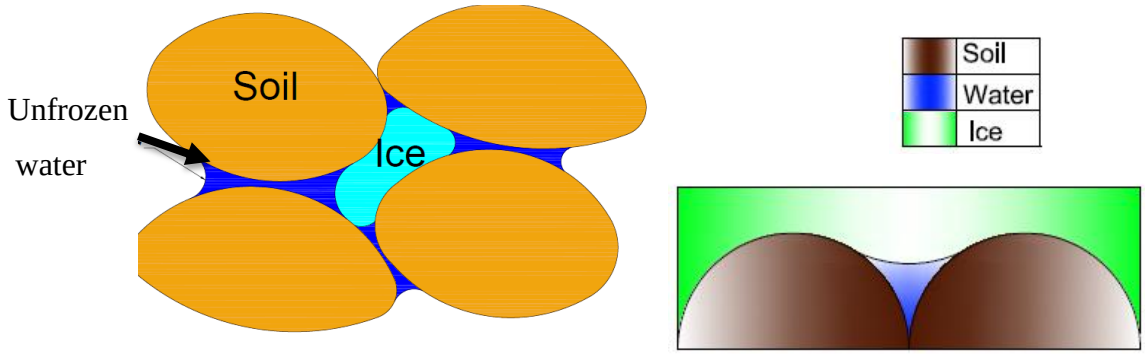

Figure 7. a) Schematic representation of frozen soils (melting may induce a significant changes of the soil structure)

The variations in the amount of ice content and the temperature are seen to affect the mechanical behavior of the frozen soil. The equilibrium between the ice and the unfrozen pore water is expressed here using the Clausius-Clapeyron equation. The equation establishes the relationship between the pressures of two phases of a single constituent material at a specified temperature. The equation is described in (9)

$$P_i = \frac{\rho_i}{\rho_l} P_l - \rho_i l \ln\left(\frac{T}{273.15}\right) \tag{9}$$

where, P_i and P_l are the pressure in the ice and water,

ρ_i and ρ_i are the densities of ice and water,

l is the latent heat of fusion (334 kJ/kg) and

T is the current temperature

The cryogenic suction, s is quantified the difference of the ice and liquid pressures.

$$s = \max\left(P_i - P_l, 0\right) \tag{10}$$

The effect of temperature of the volumetric behavior of frozen soils is now examined. Results of the various hydrostatic tests conducted on reconstituted soils (Qi et al., 2010) at varying temperatures are shown in Figure 8.a.

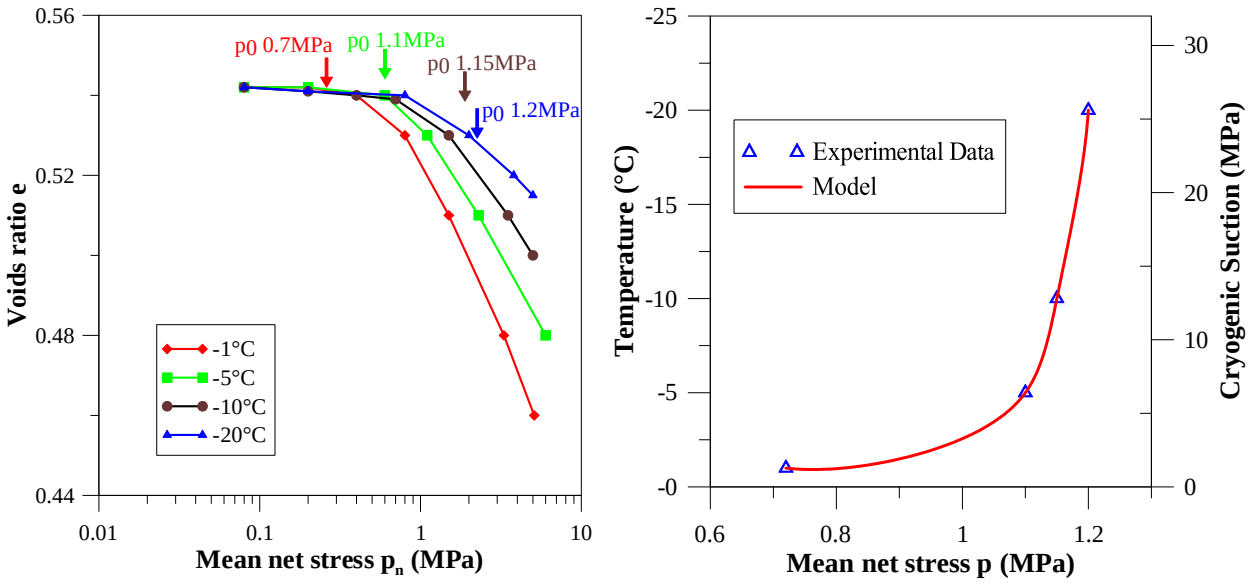

Figure 8. Mechanical behavior of frozen soils: a) effect of subzero temperature on pre-consolidation pressure and frozen soil stiffness behavior, b) variation of the pre-consolidation pressure with cryogenic suction.

The plots of the variation of the voids ratio, e vs the mean stress, p shows distinctive behaviors. The elastic slope of the curves shows a limited variation with temperature. The virgin consolidation slope however shows distinct variations as it is seen to decrease with a decrease in temperature which indicates stiffening of the soil with a reduction in temperature. An increase of the pre-consolidation stress with deceasing temperatures is evident, as shown in Figure 8.b).

Various experimental tests conducted on frozen soil have demonstrated that the mechanical behavior is influenced by temperature of the freezing environment. Figure 9.a shows the variation of the deviatoric stress with strain for triaxial test conducted on frozen soils by Parmeswaran and Jones (1981). It can be seen that the stiffness of the soil increases with decrease in temperature. It

is also observed that there is an increase in the maximum strength of the soil with decrease in temperature. The confinement pressures are also seen to affect the behavior of these sediments. Triaxial tests conducted (Parmeswaran and Jones 1981) on frozen soils with varying confining strengths have an increase in the maximum deviatoric strength observed as shown in Figure 9.b.

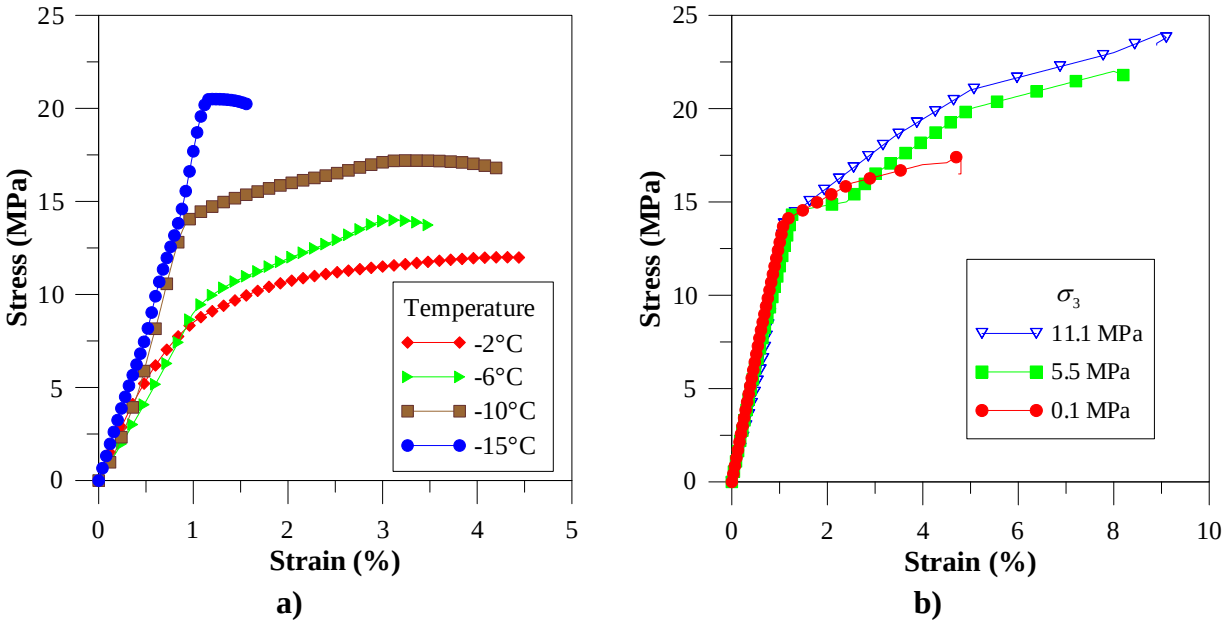

Figure 9. Variation of the stress strain behavior of reconstituted soils: a) effect of temperature, and b) effect of confining pressure

Figure 10 shows the variation of the maximum deviatoric stress with the temperature in the experiments conducted by Parmeswaran and Jones (1981). There is a linear rise in the strength of the soil with the temperature. However many observers have noted the strength increase gradually reduces with increasing temperature before reaching a constant value (Parmeswaran 1980).

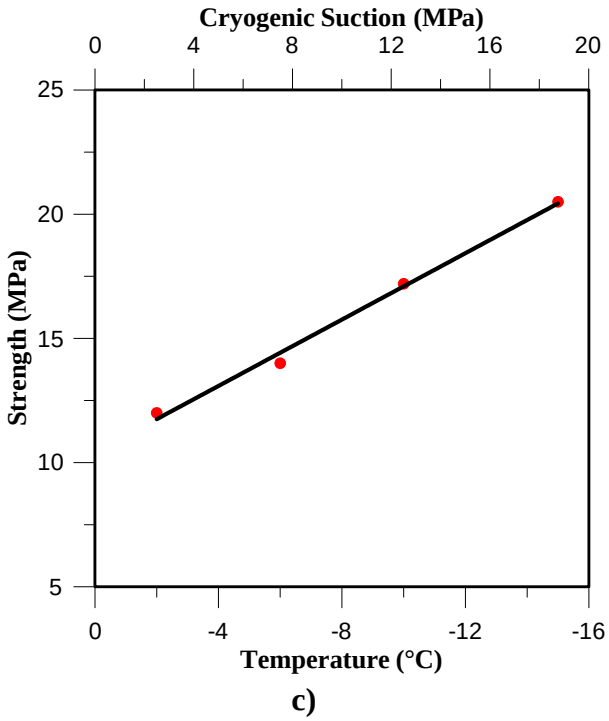

c)

Figure 10. Variation of strength with temperature

The main features of frozen soil behavior mentioned above can be included in an elasto-plastic framework based on the extension of the modified cam-clay model to accommodate for variations in temperature and cryogenic suction. Figure 11, presents the proposed yield surface to model mechanical behavior of frozen sediments. This model for frozen sediments will be validated and the presence of hydrates will be incorporated afterwards.

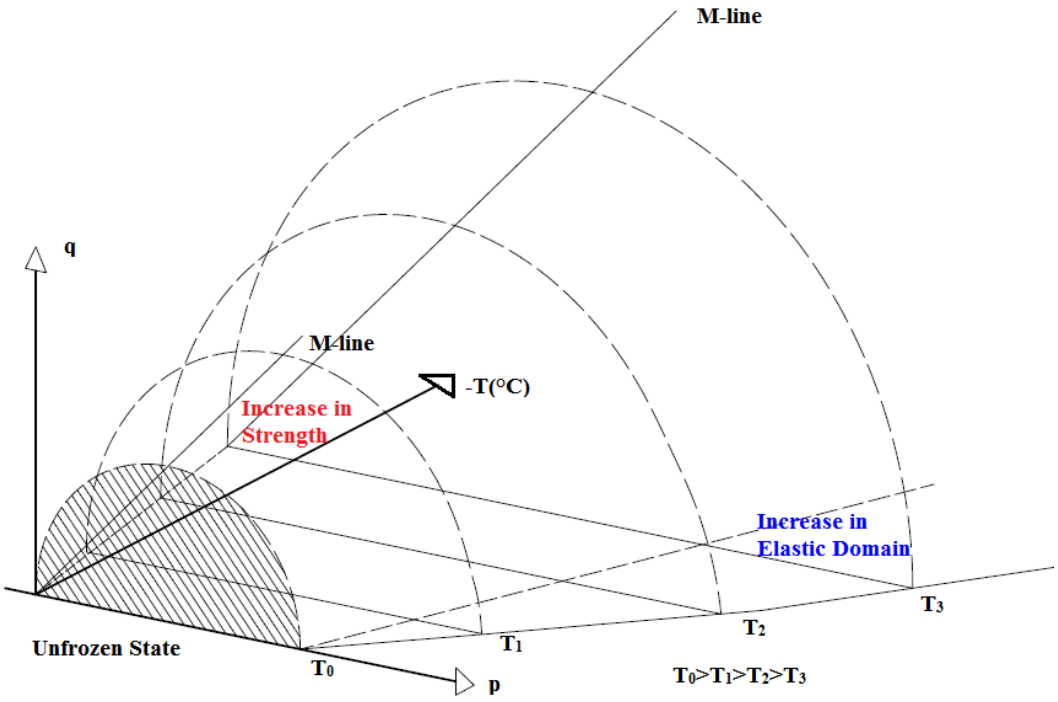

Figure 11 Idealized yield surface of a mechanical model for frozen sediments

References

Anderson, B. J., Kurihara, M., White, M. D., Moridis, G. J., Wilson, S. J., Pooladi-Darvish, M., & Boswell, R. (2011). Regional long-term production modeling from a single well test, Mount Elbert gas hydrate stratigraphic test well, Alaska North slope. *Marine and petroleum geology*, *28*(2), 493-501.

Barbour, S. L. (1998). Nineteenth Canadian Geotechnical Colloquium: The soil-water characteristic curve: a historical perspective. *Canadian Geotechnical Journal*, *35*(5), 873-894.

Beskow, G. (1935). "TJALBILDNINGEN OCH TJALLYFTNINGEN MED SARSKILD HANSYN TILL VAGAR OCH JARNVAGAR." [English translation: Soil freezing and frost heaving with special application to roads and railroads

Translated by J. O. Osterberg. Evanston, Illinois, Technological Institute,

Northwestern University, [947.] Bottero, S. (2009). Advances in the theory of capillarity in porous media. *Geologica Ultraiectina*.

Bottero, S., Hassanizadeh, S. M., Kleingeld, P. J., & Heimovaara, T. J. (2011). Nonequilibrium capillarity effects in two-phase flow through porous media at different scales. *Water Resources Research*, *47*, W10505, doi:10.1029/2011WR010887.

Celia, M. A., & Binning, P. (1992). A mass conservative numerical solution for two-phase flow in porous media with application to unsaturated flow. *Water Resources Research*, *28*(10), 2819-2828.

Celia, M. A., Bouloutas, E. T., & Zarba, R. L. (1990). A general mass-conservative numerical solution for the unsaturated flow equation. *Water resources research*, *26*(7), 1483-1496.

Chapwanya, M., & Stockie, J. M. (2010). Numerical simulations of gravity-driven fingering in unsaturated porous media using a nonequilibrium model. *Water Resources Research*, *46*, W09534, doi:10.1029/2009WR008583.

Corey, A. T. (1994). *Mechanics of immiscible fluids in porous media*. Water Resources Publication.

Dahle, H. K., Celia, M. A., & Hassanizadeh, S. M. (2005). Bundle-of-tubes model for calculating dynamic effects in the capillary-pressure-saturation relationship. *Transport in Porous media*, *58*(1-2), 5-22.

Dai, S., & Santamarina, J. C. (2013). Water retention curve for hydrate-bearing sediments. *Geophysical Research Letters*, *40*(21), 5637-5641.

Das, D. B., & Mirzaei, M. (2012). Dynamic effects in capillary pressure relationships for two‐phase flow in porous media: Experiments and numerical analyses. *AIChE Journal*, *58*(12), 3891-3903.

Diamantopoulos, E., & Durner, W. (2012a). Dynamic nonequilibrium of water flow in porous media: A review. *Vadose Zone Journal*, *11*(3).

Diamantopoulos, E., Iden, S. C., & Durner, W. (2012b). Inverse modeling of dynamic nonequilibrium in water flow with an effective approach. *Water Resources Research*, *48*(3).

Fredlund, D. G. (2000). The 1999 RM Hardy Lecture: The implementation of unsaturated soil mechanics into geotechnical engineering. *Canadian Geotechnical Journal*, *37*(5), 963-986.

Gerke, H. H., Germann, P., & Nieber, J. (2010). Preferential and unstable flow: From the pore to the catchment scale. *Vadose Zone Journal*, *9*(2), 207-212.

Glass, R. J., Steenhuis, T. S., & Parlange, J. Y. (1989). Mechanism for finger persistence in homogeneous, unsaturated, porous media: Theory and verification. *Soil Science*, *148*(1), 60-70.

Hassanizadeh, S. M., & Gray, W. G. (1993). Thermodynamic basis of capillary pressure in porous media. *Water Resources Research*, *29*(10), 3389-3405.

Hassanizadeh, S. M., Celia, M. A., & Dahle, H. K. (2002). Dynamic effect in the capillary pressure–saturation relationship and its impacts on unsaturated flow. *Vadose Zone Journal*, *1*(1), 38-57.

Homsy, G. M. (1987). Viscous fingering in porous media. *Annual Review of Fluid Mechanics*, *19*(1), 271-311.

Jang, J., & Santamarina, J. C. (2014). Evolution of gas saturation and relative permeability during gas production from hydrate-bearing sediments: Gas invasion vs. gas nucleation. *Journal of Geophysical Research: Solid Earth*.

Joekar-Niasar, V., & Majid Hassanizadeh, S. (2011). Effect of fluids properties on non-equilibrium capillarity effects: Dynamic pore-network modeling. *International Journal of Multiphase Flow*, *37*(2), 198-214.

Johnson, A., Patil, S., & Dandekar, A. (2011). Experimental investigation of gas-water relative

permeability for gas-hydrate-bearing sediments from the Mount Elbert Gas Hydrate Stratigraphic Test Well, Alaska North Slope. *Marine and petroleum geology*, *28*(2), 419-426.

Kimoto, S., Oka, F., Fushita, T., & Fujiwaki, M. (2007). A chemo-thermo-mechanically coupled numerical simulation of the subsurface ground deformations due to methane hydrate dissociation. *Computers and Geotechnics*, *34*(4), 216-228.

Klar, A., Soga, K., & Ng, M. Y. A. (2010). Coupled deformation–flow analysis for methane hydrate extraction. *Geotechnique*, *60*(10), 765-776.

Konrad, J. M., and Morgenstern, N.R., 1980. A mechanistic theory of ice lens formation in fine-grained soils. Canadian Geotechnical Journal 174, 473-486.

Kueper, B. H., & Frind, E. O. (1991). Two-phase flow in heterogeneous porous media: 1. Model development. *Water Resources Research*, *27*(6), 1049-1057.

Kumar, A., Maini, B., Bishnoi, P. R., Clarke, M., Zatsepina, O., & Srinivasan, S. (2010). Experimental determination of permeability in the presence of hydrates and its effect on the dissociation characteristics of gas hydrates in porous media. *Journal of Petroleum Science and Engineering*, *70*(1), 114-122.

Leverett, M. C. (1941). Capillary behavior in porous solids. *Trans. Am. Inst.*

Liu, X., & Flemings, P. B. (2007). Dynamic multiphase flow model of hydrate formation in marine sediments. *Journal of Geophysical Research: Solid Earth (1978–2012)*, *112*(B3).

Liu, Y., Steenhuis, T. S., & Parlange, J. (1994). Formation and persistence of fingered flow fields in coarse grained soils under different moisture contents. *Journal of hydrology*, *159*(1), 187-195.

Løvoll, G., Jankov, M., Måløy, K. J., Toussaint, R., Schmittbuhl, J., Schäfer, G., & Méheust, Y. (2011). Influence of viscous fingering on dynamic saturation–pressure curves in porous media. *Transport in porous media*, *86*(1), 305-324.

Manthey, S., Hassanizadeh, S. M., Helmig, R., & Hilfer, R. (2008). Dimensional analysis of two-phase flow including a rate-dependent capillary pressure–saturation relationship. *Advances in water resources*, *31*(9), 1137-1150.

Miller, R. D., 1978. Frost heaving in non-colloidal soils. Third International Conference on Permafrost Natural Resources. Council of Can.Edmonton, Alta

Mirzaei, M., & Das, D. B. (2007). Dynamic effects in capillary pressure–saturations relationships for two-phase flow in 3D porous media: Implications of micro-heterogeneities. *Chemical engineering science*, *62*(7), 1927-1947.

Mualem, Y. (1976). A new model for predicting the hydraulic conductivity of unsaturated porous media. *Water resources research*, *12*(3), 513-522.

Multon, S., Sellier, A., and Perrin, B., 2012. Numerical analysis of frost effects in porous media. Benefits and limits of the finite element poroelasticity formulation. International journal for numerical and analytical methods in geomechanics. 364. 438-458.

Nieber, J. L., Dautov, R. Z., Egorov, A. G., & Sheshukov, A. Y. (2005). Dynamic capillary pressure mechanism for instability in gravity-driven flows; review and extension to very dry conditions. *Transport in porous media*, *58*(1-2), 147-172.

O'Carroll, D. M., Phelan, T. J., & Abriola, L. M. (2005). Exploring dynamic effects in capillary pressure in multistep outflow experiments. *Water resources research*, *41*(11).

Parameswaran, V., and Jones, S., 1981. Triaxial testing of frozen sand. Journal of Glaciology 27(95), 147-155

Qi, J., Hu, W., and Ma, W., 2010. Experimental study of a pseudo-preconsolidation pressure in frozen soils. Cold Regions Science and Technology, 60(3), 230-233

Ross, P. J., & Smettem, K. R. J. (2000). A simple treatment of physical nonequilibrium water flow in soils. *Soil Science Society of America Journal*, *64*(6), 1926-1930.

Ruan, X., Song, Y., Liang, H., Yang, M., & Dou, B. (2012). Numerical simulation of the gas production behavior of hydrate dissociation by depressurization in hydrate-bearing porous medium. *Energy & Fuels*, *26*(3), 1681-1694.

Rutqvist, J., & Moridis, G. J. (2009). Numerical studies on the geomechanical stability of hydrate-bearing sediments. *Spe Journal*, *14*(02), 267-282.

Sanchez, M., & Shastri, A., Santamarina, J. C. (2013). Modeling gas hydrate bearing sediments using a coupled approach. In *1st Pan-American Conference on Unsaturated Soils*.

Sander, G. C., Glidewell, O. J., & Norbury, J. (2008, November). Dynamic capillary pressure,

hysteresis and gravity-driven fingering in porous media. In *Journal of Physics: Conference Series* (Vol. 138, No. 1, p. 012023). IOP Publishing.

Schultze, B., O. Ippisch, B. Huwe, and W. Durner. (1999). Dynamic nonequilibrium in unsaturated water flow. In:M.Th. van Genuchten et al., editors, Proceedings of an International Workshop on Characterization and Measurement of the Hydraulic Properties of Unsaturated Porous Media, Riverside, CA. 22–24 Oct. 1997. Univ. of California, Riverside. p. 877–892.

Seol, Y., & Kneafsey, T. J. (2011). Methane hydrate induced permeability modification for multiphase flow in unsaturated porous media. *Journal of Geophysical Research: Solid Earth (1978–2012)*, *116*(B8).

Sun, X., Nanchary, N., & Mohanty, K. K. (2005). 1-D modeling of hydrate depressurization in porous media. *Transport in Porous Media*, *58*(3), 315-338.

Taber, S., 1929. Frost heaving. The Journal of Geology, 428-461.

Tice, A. R., Anderson, D. M., and Banin, A. (1976) "The prediction of unfrozen water contents in frozen soils from liquid limit determinations." Proc., Symposium on Frost Action on Roads, Paris (1976).

Tice, A., Black, P., and Berg, R., 1988. Unfrozen water contents of undisturbed and remolded Alaskan silt. Cold Regions Science and Technology, 17(2), 103-111

Topp, G. C., Klute, A., & Peters, D. B. (1967). Comparison of water content-pressure head data obtained by equilibrium, steady-state, and unsteady-state methods. *Soil Science Society of America Journal*, *31*(3), 312-314.

van Genuchten, M. T. (1980). A closed-form equation for predicting the hydraulic conductivity of unsaturated soils. *Soil Science Society of America Journal*, *44*(5), 892-898.

Vanapalli, S. K., Fredlund, D. G., Pufahl, D. E., & Clifton, A. W. (1996). Model for the prediction of shear strength with respect to soil suction. *Canadian Geotechnical Journal*, *33*(3), 379-392.

Vereecken, H., Kasteel, R., Vanderborght, J., & Harter, T. (2007). Upscaling hydraulic properties and soil water flow processes in heterogeneous soils. *Vadose Zone Journal*, *6*(1), 1-28.

Wildenschild, D., Hopmans, J. W., & Simunek, J. (2001). Flow rate dependence of soil hydraulic characteristics. *Soil Science Society of America Journal*, *65*(1), 35-48.

Wildenschild, D., Hopmans, J. W., Rivers, M. L., & Kent, A. J. R. (2005). Quantitative analysis of flow processes in a sand using synchrotron-based X-ray microtomography. *Vadose Zone Journal*, *4*(1), 112-126.

White, K. D. (1999). "Hydraulic and physical properties affecting ice jams." DTIC Document.

.

PRODUCTS

Publications – Presentations:

- A poster was presented during to the Gordon Research Conference on Natural Gas Hydrate Systems hold in Galveston, Texas, March, 2014. Title: "Numerical THCM Modeling of HBS using a truly coupled approach"
- A conference paper has been accepted for the 14th IACMAG (International Conference of the International Association for Computer Methods and Advances in Geomechanics). Kyoto Japan 22-25 September 2014 Title: "Coupled Modeling of Gas Hydrate Bearing Sediments". Authors: M. Sanchez, J. C. Santamarina. A. Shastri & Xuerui Gai.

Website: Publications (for academic purposes only) and key presentations are included in http://pmrl.ce.gatech.edu/; http://engineering.tamu.edu/civil/people/msanchez

Technologies or techniques: None at this point.

Inventions, patent applications, and/or licenses: None at this point.

Other products: None at this point.

PARTICIPANTS

Research Team: The current team is shown next.

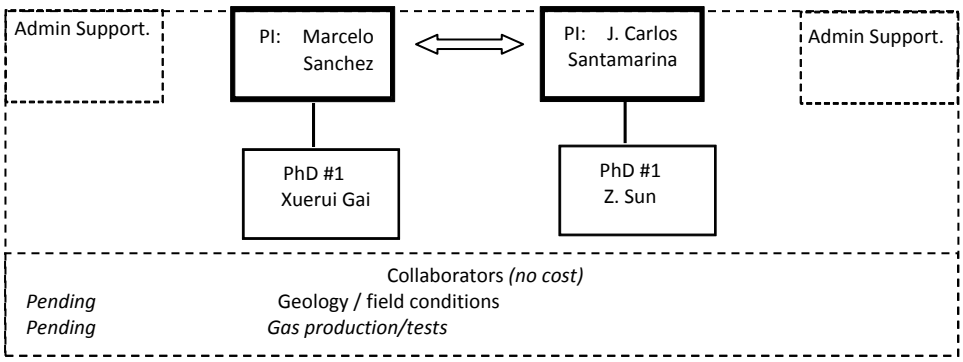

IMPACT

- While it is still too early to assess impact, we can already highlight the computational platform extensively validated in a wide range of coupled thermo-hydro-chemo-mechanical coupled problems (CB_Hydrate).

CHANGES/PROBLEMS:

None so far.

SPECIAL REPORTING REQUIREMENTS:

Nothing to report

BUDGETARY INFORMATION:

TAMU

Grant No.DE-FE0013889 — **EXHIBIT 2- COST PLAN/STATUS**

TEES Project 32525-C3870 CE

COST PLAN/STATUS

	Budget Period 1								Budget Period 2							
	Q1		Q2		Q3		Q4		Q1		Q2		Q3		Q4	
	Enter date range		Enter date range		Enter date range		Enter date range		Enter date range		Enter date range		Enter date range		Enter date range	
Baseline Reporting Quarter	10/1/13-12/31/14		01/01/14-03/31/14		04/01/14-06/30/14		07/01/14-9/30/14									
	Q1	Cumulative Total	Q2	Cumulative Total	Q3	Cumulative Total	Q4	Cumulative Total	Q1	Cumulative Total	Q2	Cumulative Total	Q3	Cumulative Total	Q4	Cumulative Total
Baseline Cost Plan	$ 30,300.00	$ 30,300.00	$ 60,600.00	$ 90,900.00												
Federal Share	$ 30,300.00	$ 30,300.00	$ 60,600.00	$ 90,900.00												
Non-Federal Share	$ 11,223.00	$ 11,223.00	$ 11,223.00	$ 22,446.00												
Total Planned	$ 41,523.00	$ 41,523.00	$ 71,823.00	$ 113,346.00												
Actual Incurred Costs	$ 5,301.83	$ 5,301.83	$ 13,764.34	$ 19,066.17												
Federal Share	$ 3,335.02	$ 3,335.02	$ 13,183.70	$ 16,518.72												
Non-Federal Share	$ 5,182.94	$ 5,182.94	$ 25,938.52	$ 31,121.46												
Total Incurred costs	$ 8,517.96	$ 8,517.96	$ 39,122.22	$ 47,640.18												
Varience	$ 33,005.04	$ 33,005.04	$ 32,700.78	$ 65,705.82												
Federal Share	$ 1,966.81	$ 1,966.81	$ 5,882.47	$ 7,849.28												
Non-Federal Share	$ 6,040.06	$ 6,040.06	$ 6,040.06	$ 12,080.12												
Total Varience	$ 8,006.87	$ 8,006.87	$ 11,922.53	$ 19,929.40												

GT

	Budget Period 1								Budget Period 2							
	Q1		Q2		Q3		Q4		Q1		Q2		Q3		Q4	
Baseline Reporting Quarter	10/1/13 - 12/31/13		1/1/14 - 3/31/14		4/1/14 - 6/30/14		7/1/14 - 9/30/14		10/1/14 - 12/31/14		1/1/15 - 3/31/15		4/1/15 - 6/30/15		7/1/15 - 9/30/15	
	Q1	Cumulative Total	Q2	Cumulative Total	Q3	Cumulative Total	Q4	Cumulative Total	Q1	Cumulative Total	Q2	Cumulative Total	Q3	Cumulative Total	Q4	Cumulative Total
Baseline Cost Plan																
Federal Share	18,000	18,000	18,000	36,000	18,000	54,000	32,223	86,223	18,000	104,223	18,000	122,223	18,000	140,223	34,658	174,881
Non-Federal Share	6,119	6,119	6,119	12,238	6,119	18,357	10,954	29,262	6,119	35,381	6,119	41,500	6,119	47,619	11,782	59,401
Total Planned	24,119	24,119	24,119	48,238	24,119	72,357	43,177	115,485	24,119	139,604	24,119	163,723	24,119	187,842	46,440	234,282
Actual Incurred Cost																
Federal Share	0	0	**13,164**	13,164												
Non-Federal Share	0	0	6,119	6,119												
Total Incurred Costs	0	0	19,283	19,283												
Variance																
Federal Share	-18,000	-18,000	-4,836	-22,836												
Non-Federal Share	-6,119	-6,119	0	-6,119												
Total Variance	-24,119	-24,119	-4,836	-28,955												

National Energy Technology Laboratory

626 Cochrans Mill Road
P.O. Box 10940
Pittsburgh, PA 15236-0940

3610 Collins Ferry Road
P.O. Box 880
Morgantown, WV 26507-0880

13131 Dairy Ashford Road, Suite 225
Sugar Land, TX 77478

1450 Queen Avenue SW
Albany, OR 97321-2198

Arctic Energy Office
420 L Street, Suite 305
Anchorage, AK 99501

Visit the NETL website at:
www.netl.doe.gov

Customer Service Line:
1-800-553-7681